

# **A NEW POWERFUL TOOL FOR INTERPRETING AND PREDICTING IN RESERVOIR GEOPHYSICS: THEORETICAL MODELING AS APPLIED TO LABORATORY MEASUREMENTS OF THERMAL PROPERTIES**

Irina Bayuk, Yuri Popov, and Anton Parshin  
Schlumberger Moscow Research Center, Moscow, Russia

*This paper was prepared for presentation at the International Symposium of the Society of Core Analysts held in Austin, Texas, USA 18-21 September, 2011*

## **ABSTRACT**

This paper demonstrates new possibilities provided by a combination of effective medium theory (EMT) with laboratory experiment on thermal properties of porous-cracked rocks. Such a combination can solve many actual problems in petrophysics and prospecting geophysics including EMT-based inversion of pore/crack geometry and thermal conductivity (TC) of mineral matrix from TC measurements on samples saturated with different fluids. The inverted geometry is used for EMT-based prediction of the other physical properties (elastic wave velocities and coefficient of linear thermal expansion). The opposite procedure is also applied — TC prediction from measurements of elastic wave velocities and electrical resistivity. An example is presented of reconstructing the TC distribution along a well from sonic, density, and porosity logs. The theoretical modeling is shown to be a useful tool in solving the ‘oil-in-place’ problem from measurements on density, volumetric heat capacity, and porosity. The EMT is used to reconstruct the distribution functions of pore/crack volume over aspect ratio before and after experiment at elevated pressure and temperature (PT) conditions and reveal principal factors controlling the TC change at these conditions.

## **INTRODUCTION**

Knowledge of thermal properties (thermal conductivity and diffusivity and volumetric heat capacity) of porous-cracked rocks is of great importance today; these properties are widely applied in different areas including prospecting geophysics, exploitation of hydrothermal resources, storage of radioactive materials, *etc.* Different experimental techniques allow one to measure rock’s thermal properties in laboratory at the standard (20°C and 1 atm) and *in situ* conditions [1]. However, in field practice, the rock’s thermal properties are related to “nonmeasurable” properties. These facts lead to a necessity to develop theoretical approaches of the thermal property’s prediction.

A porous-cracked rock can be considered as a microheterogeneous medium whose heterogeneities are particles of mineral material, pores, and cracks filled with various

fluids and melt. In this case, the rock's physical properties, elastic and transport (thermal and electrical conductivity, hydraulic permeability, and permittivity) are coordinate-dependent. In the case of thermal properties, according to the Fourier law, the density of thermal flux observed at a given depth is governed by the temperature gradient and TC of the rock through which the flux passes  $\mathbf{q}(\mathbf{r}) = -\boldsymbol{\lambda}(\mathbf{r})\nabla T(\mathbf{r})$ , where  $\mathbf{q}(\mathbf{r})$  is the vector of the thermal flux density,  $\boldsymbol{\lambda}(\mathbf{r})$  is the TC of rock that is a tensor of the second rank,  $\nabla T(\mathbf{r})$  is the temperature gradient vector, and  $\mathbf{r}$  is a point in rock volume. If the heterogeneity size is small compared to the distance at which the temperature difference is analyzed, and the medium is statistically homogeneous, the rock can be considered as macrohomogeneous, having thermal conductivity  $\boldsymbol{\lambda}^*$  (so-called, effective TC) relating the thermal flux density and temperature gradient averaged over a representative equivalent volume (REV). The REV is assumed to have the same properties as rock in a whole (at scale of the problem consideration). The Fourier law for the medium with effective TC has the form  $\langle \mathbf{q}(\mathbf{r}) \rangle = -\boldsymbol{\lambda}^* \langle \nabla T(\mathbf{r}) \rangle$ . The angular brackets mean averaging over the REV. The effective TC can be calculated using the EMT methods [1]. In addition, EMT is applicable for simultaneous calculation of the effective elastic and transport properties including the electrical, hydraulic, and thermal conductivity [2, 3]. In this paper we demonstrate new possibilities in solving different geophysical problems that result from a combination of EMT with laboratory measurements of the thermal properties.

## A UNIFIED APPROACH FOR CALCULATING THE EFFECTIVE ELASTIC AND TRANSPORT PROPERTIES BASED ON THE EFFECTIVE MEDIUM THEORY

According to the EMT-based approach, each inclusion (particle of mineral material, pore or crack) is assumed to be of elliptical shape (general ellipsoid) and is embedded in a medium called "comparison body" having properties  $\mathbf{X}^c$ . The assumption of elliptical shape allows one to obtain a solution in an analytical form. For the tensor of effective elastic or transport properties ( $\mathbf{X}^*$ ) we have

$$\mathbf{X}^* = \langle \mathbf{X}(\mathbf{r}) [\mathbf{X}^c(\mathbf{I} - \mathbf{F}) + \mathbf{X}(\mathbf{r})\mathbf{F}]^{-1} \rangle \langle [\mathbf{X}^c(\mathbf{I} - \mathbf{F}) + \mathbf{X}(\mathbf{r})\mathbf{F}]^{-1} \rangle^{-1}, \quad (1)$$

where the angular brackets mean volume averaging,  $\mathbf{X}$  is the second-rank tensor of thermal, electrical or hydraulic conductivity, or the fourth-rank effective stiffness tensor;  $\mathbf{I}$  is the unit tensor. For the transport properties  $\mathbf{F}$  is the depolarization factor introduced by Landau and Lifshitz [4] and the Eshelby tensor in the case of elasticity [5]. This tensor is calculated by the formula  $\mathbf{F} = -\mathbf{X}^c \mathbf{g}$ . The tensor  $\mathbf{g}$  depends on the properties of comparison body and pore/crack geometry, and formulas for its calculation for the both elastic and transport properties can be found in [2]. We assume that the inclusions are different in shape, orientation, and physical properties. The shape of inclusions is modeled by ellipsoids of revolution. In this case, averaging in equation 1 is performed over the rock's composition using the distribution function of inclusion's volume over their aspect ratio and orientation. The comparison body in formula 1 is assumed to be

arbitrary and should be chosen to reflect the inner structure. If the properties of the comparison body are set equal to effective properties (i.e.,  $\mathbf{X}^c = \mathbf{X}^*$ ) we have formulas of the self-consistent approach [1].

Unified equation 1 gives a possibility to determine one type of physical properties from another, since all the aforesaid properties are controlled by one and the same inner structure. For example, we can determine the TC from elastic wave velocities, or from electrical resistivity, and vice versa.

## **NEW POSSIBILITIES OF EXPERIMENTAL STUDY COMPLEMENTED BY THEORETICAL MODELING**

### **Inversion of Pore-Crack Geometry and TC of Mineral Matrix**

We consider a collection of limestone samples from an oilfield. The optical scanning method is applied for experimental study [1]. The natural liquids filling the pore space of samples were removed by extracting and heating, and the TC was measured on dry samples. Then, the samples were vacuum saturated with distilled water and, then, with ethylene-glycol, and the TC was measured on the liquid-saturated samples.

Before applying the EMT-based formulas to invert the pore-crack geometry from the TC measurements, a model of porous-cracked rock should be constructed. The model depends on the reservoir type and should reflect its specific features. The shape of pores and cracks is assumed to be the ellipsoid of revolution. Since the TC measurements exhibit no anisotropy, we assume that the inclusions are chaotically oriented in space. The shape of particles of mineral material is set to be spherical. To describe the distribution of pore/crack volume over aspect ratios we use the two-parametric Beta-distribution function (DF) over the depolarization factor:

$$P(F) = \frac{\Gamma(\alpha+\beta)}{\Gamma(\alpha)\Gamma(\beta)} F^{\alpha-1} (1-F)^{\beta-1} \quad (2)$$

with non-negative parameters  $\alpha$  and  $\beta$ ;  $\Gamma$  is the gamma function. We use this DF because its shape is very flexible and depending on the parameters may be similar to the shape of lognormal distribution or uniform distribution, or may provide maxima in the domain of very thin cracks or open pores. The parameters in the DF are assumed to be unknown. The mineral material (or matrix) in our model is represented by the mineral grains, residuals of organic matter, capillary water, and isolated pores amounting up to 40% of the total porosity in carbonate reservoirs. The TC of matrix is also assumed to be unknown. This model contains three unknowns to be inverted from the experimental data. The unknowns are found by minimizing the sum of squared differences between the experimental and theoretical values of physical properties  $\mathbf{X}^*$  (calculated by equation 1) normalized by the respective experimental values. Use of such a normalized function for the minimization is helpful if the inversion is performed simultaneously from different physical properties.

The comparison body is set to be equal to the body with the effective properties. Since, in the general case, a solution to the inverse problem is nonunique, physically plausible bounds are imposed on the unknown parameters, which allow one to obtain more realistic solution. Thus, the matrix TC varies around a value corresponding to the TC of calcite [3.0 W/(m·K)]. The parameters of the Beta-distribution function are assumed to vary from 0.0001 to 200. Figure 1 shows examples of the DFs inverted for samples having different porosity in comparison to the photos of the cubic sample sides (3 by 3 cm) saturated with fluorescent dye. As seen from the photo of sample with 1.2%-porosity (Figure 1a), cracks dominate, and this fact is well reflected by the inverted DF exhibiting cracks with the aspect ratio maximum around 0.02. For the sample having 5.8-% porosity, the photo demonstrates more isometric pores (Figure 1b). This fact is well reflected by the DF having the aspect ratio maximum around 0.1. The TC of matrix resulting from the inversion is 3.0 and 3.1 W/(m·K) for these two samples, respectively. The distribution of inverted matrix TC against porosity for samples of this collection is shown in Figure 1c.

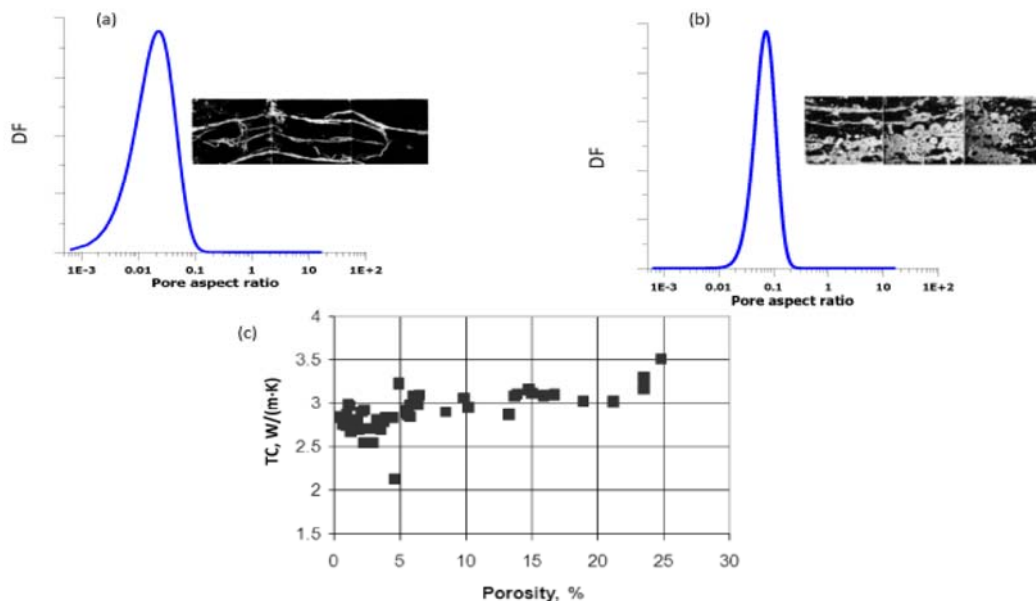


Figure 1. Photos of cubic sample sides and inverted DFs of limestone samples. (a) cracked sample of 1.2-% porosity (b) porous-cracked sample of 5.8-% porosity; (c) matrix thermal conductivity inverted from the measurements.

### Prediction of TC from Other Physical Properties and Vice Versa

The approach based on rock's microstructure inversion is used to predict one type of properties from another. We apply EMT to invert the pore/crack geometry from elastic wave velocities and electrical resistivity. Then, the inverted values together with the TC

of components are used to predict the TC of rock under the same conditions as measured physical properties. In the inversion, the self-consistent scheme is applied.

This approach is tested on samples of Yucatan organogenic limestones. For these samples the porosity, density, elastic wave velocities ( $V_p$  and  $V_s$ ), thermal and electrical conductivity were measured in laboratory (the measurements of elastic and electrical properties were provided by TU of Berlin). Figure 2a shows the results of TC prediction together with experimental data for the limestone samples fully saturated with water. For experimental values 10-% error bars are plotted. Two variants of inversion of pore/crack geometry are used. In the first variant only elastic wave velocities are taken for the inversion. In the second variant, the pore/crack geometry and matrix TC were inverted from the both elastic properties and electrical resistivity using nonlinear minimization described in the previous section. A calculation by the Lichteneker method [6] that does not take into account the pore/crack geometry is also shown. The linear trends are plotted for experimental values and different theoretical predictions. As seen, the inversion from a combination of data on elasticity and electrical resistivity produces the closest values to experimental ones. All predicted values are within the domain restricted by 10-% error bars. The average difference between the theoretical and experimental values is around 5%. Moreover, the linear trend corresponding to TC values found from this inversion is parallel to the experimental trend. The DFs derived from the different properties and combinations of them look very similar. An example of such a DF derived from combination of elastic properties and electrical resistivity is shown in Figure 2b. An inverse procedure — prediction of elastic wave velocities from TC measurements is also carried out. The predicted velocities are in good agreement with experimental data.

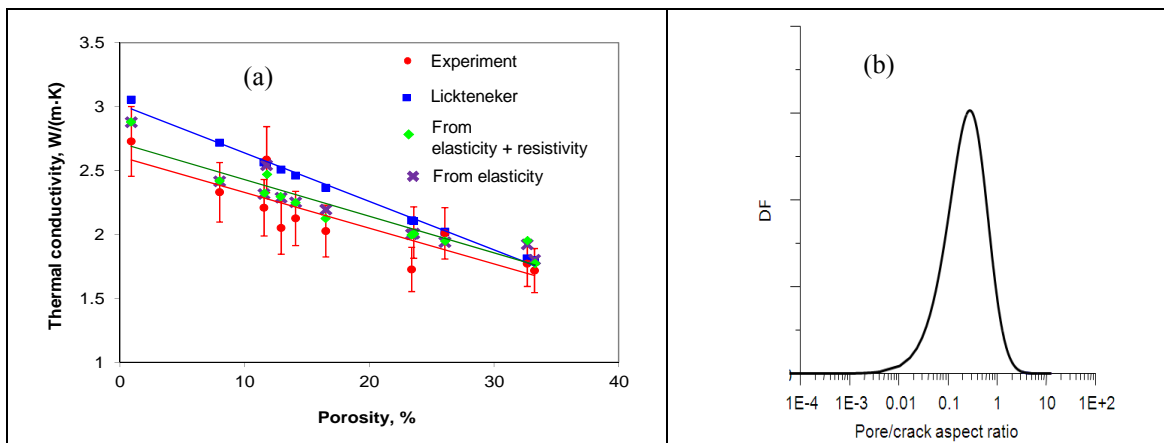


Figure 2. (a) Thermal conductivity of limestone vs porosity: experimental values, theoretically predicted values from elastic and electrical properties, and values calculated with the Lichteneker method: (b) an example of DF inverted from combination of elastic properties and electrical resistivity for sample of 11.5-% porosity.

Figure 3 demonstrates an inversion of TC from logging data on sonic velocities ( $V_p$  and  $V_s$ ), porosity, density, and water-saturation for a well penetrating a carbonate reservoir (composed of limestone). For this depth interval, 100-% water-saturation is indicated. TC

values measured at standard conditions in laboratory on samples fully saturated with water, which were extracted from related depths, are shown for comparison. As seen, the predicted TC values are within the 10-% error domain shown for experimental TC except for three upper points. However, a systematic difference between the experimental and predicted TC values exists: the predicted values are smaller than those measured in laboratory. Note that the temperature dependence of calcite was not taken into account for such a prediction. Besides, porosity at *in situ* conditions can be smaller than that at the standard conditions. Finally, the physical properties of rocks are different at different scale. All these factors may contribute to this difference between the TC values.

### Prediction of Coefficient of Linear Thermal Expansion from TC Measurements

The simplest model that can be suggested for sedimentary rock is a two-phase medium including the particles of mineral material and voids (pores and cracks). As follows from derivations of Shermegor [7], in the case of two-phase isotropic medium, the linear coefficient of thermal expansion (CLTE) can be calculated by the formula

$$\alpha^* = \langle \alpha \rangle + (\alpha_1 - \alpha_2) [(K^*)^{-1} - K_R^{-1}] / (K_1^{-1} - K_2^{-1}). \quad (3)$$

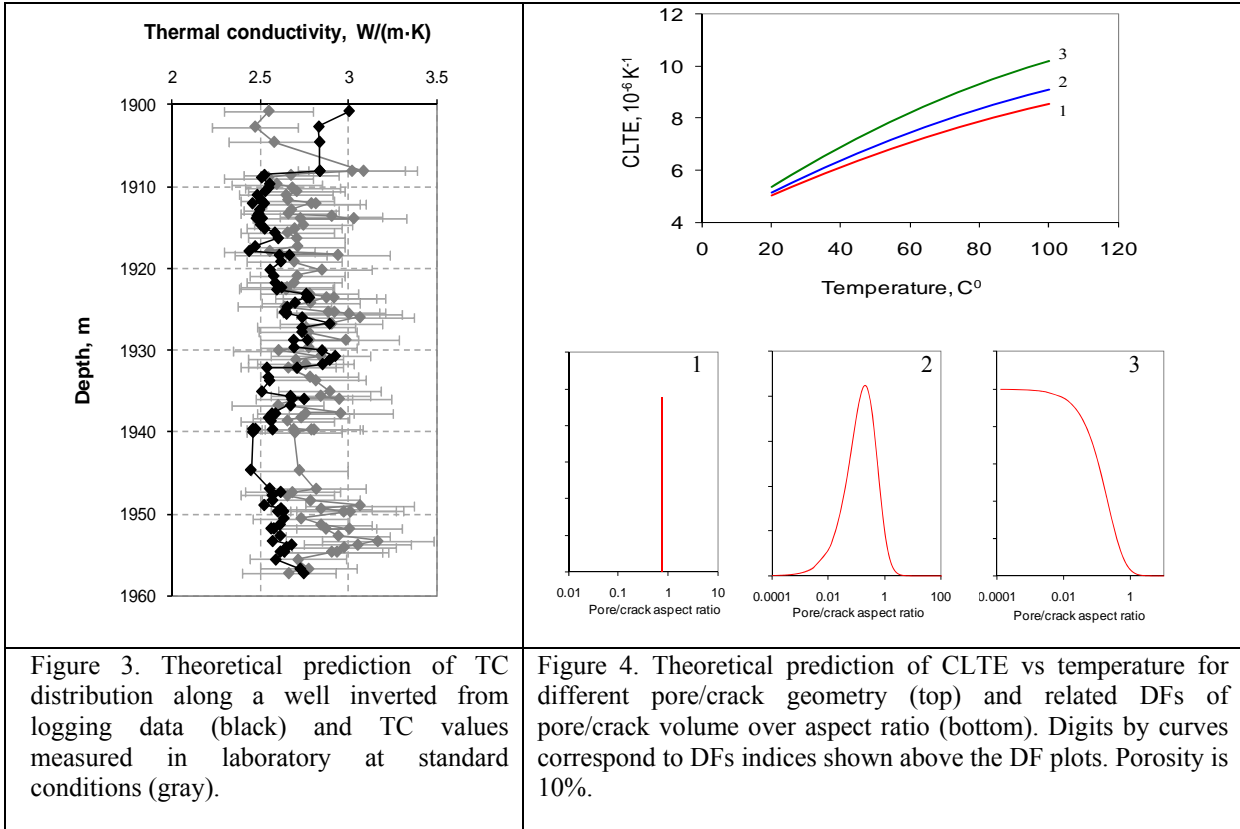
Here,  $\alpha_1$  and  $\alpha_2$  are the CLTE of mineral matrix and filling material;  $K_1$  and  $K_2$  are, respectively, the elastic bulk moduli of components;  $K_R$  is the bulk modulus of the two-phase medium calculated by the Reuss method:  $K_R = \langle K^{-1} \rangle^{-1}$ ;  $K^*$  is the effective elastic bulk modulus.

### Theoretical Prediction of CLTE Temperature Dependence of Isotropic Carbonate Rocks

We use formula 3 to predict CLTE vs temperature for water-saturated limestone having different porosity and pore/crack geometry (Figure 4). According to experimental study [8, 9], temperature slightly changes the elastic properties of mineral material and water in a range up to 100°C. Thus, the bulk modulus of calcite decreases only by 3%. The bulk modulus of water varies from 2.03 to 2.19 GPa in this range. Consequently, the bulk moduli of these constituents can be taken as equal to those at standard conditions (i.e., 75 GPa for calcite and 2.08 GPa for water). The CLTE of limestone at standard conditions and its temperature dependence are taken from [8] and [10]. The following types of pore/crack shape are considered (Figure 4, bottom): (1) all pores are spheres, (2) the pore/crack volume distribution over aspect ratio with DF maximum around aspect ratio 0.04 (derived from the TC measurements described in the previous section for a sample having the porosity 10%), and (3) the pore/crack volume distribution over aspect ratio is described by the DF with maximum in the crack domain. The pores and cracks are assumed to be chaotically oriented in rock volume. The self-consistent scheme is applied to find the effective bulk modulus.

As known from theoretical modeling of elastic properties, enhanced amount of cracks lowers the bulk modulus. Therefore, according to equation 3, the maximum CLTE is reasonably observed for more cracked rocks (crack system (3)), and CLTE for crack

system (1) should be the smallest of the three cases. The CLTE difference for DFs (1) and (3) attains 20% at temperature 100° C. Our theoretical modeling also shows that for DF of type (2) shown in Figure 4 and temperature range 20 – 100° C, the CLTE of limestone changes up to three times as porosity increases from 0 to 30%.



CLTE Calculations for Anisotropic Media

In the case of anisotropic rock, the effective CLTE is calculated by the formula [7]

$$\alpha^e = \langle \alpha_v B_v \rangle, B_v = C_v (I - g C^e)^{-1} \langle (I - g C^e)^{-1} \rangle^{-1} S^*, C^e = C - C^p. \quad (4)$$

The relation for  $B_v$  in this formula follows from the Eshelby solution [5]. Here,  $C$  is the stiffness tensor,  $I$  is the fourth-rank unit tensor, and  $S^*$  is the effective compliance tensor. Formula 4 takes into account the pore/crack geometry and peculiarities in connections of components and allows one to incorporate the anisotropy caused by preferred orientation of the both mineral grains and cracks. The number of components composing a rock can be arbitrary.

We apply formula 4 to analyze the effect of vertical water-saturated cracks on CLTE anisotropy of limestone. The CLTE vs crack volume calculated for the vertical and lateral directions in the water-saturated limestone is shown in Figure 5a. The CLTE in the

vertical direction is smaller than that in the lateral direction. This is explained by that the rock with vertical parallel cracks is stiffer in the vertical direction compared to lateral one. As seen, 1% of water-saturated vertical cracks of aspect ratio 0.005 results in 15% of the CLTE anisotropy (Figure 5b) calculated as  $\frac{CLTE_{\max}}{CLTE_{\min}}$ .

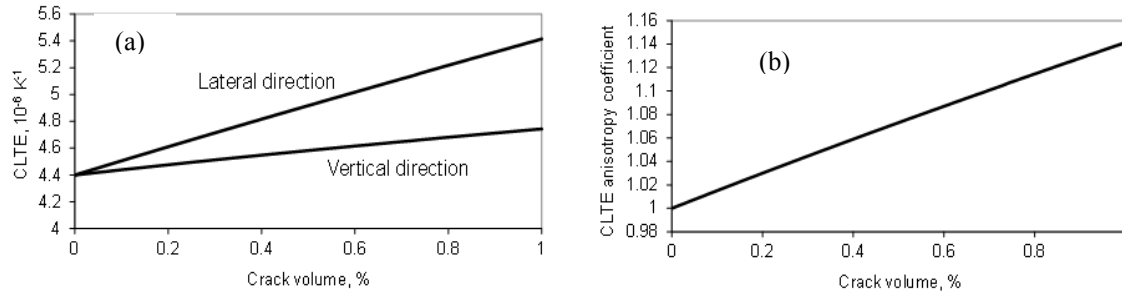


Figure 5. (a) Theoretical prediction of CLTE of water-saturated limestone vs crack volume in the lateral and vertical directions and (b) anisotropy coefficient of CLTE vs crack volume.

### Solution of ‘Oil-in-Place’ Problem with the Help of Theoretical Modeling

The theoretical modeling is helpful in solving the so-called ‘oil-in-place’ problem arising during hydrocarbon recovery. This problem assumes estimation of residual oil content in a reservoir. We suggest solving this problem from measurements of porosity, density, and volumetric heat capacity (VHC) of rock. In addition, the rock’s lithology should be known. The VHC and density are two “lucky” properties whose theoretical prediction from the composition gives an exact solution as opposed to problems of elastic and transport properties estimation. In order to find the oil content the following system should be solved relative four unknowns  $\phi_m$ ,  $\phi_g$ ,  $\phi_w$ , and  $\phi_o$  that are, respectively, the volume concentrations of mineral matrix, gas, water, and oil:

$$\begin{aligned} C^* &= \phi_m C_m + \phi_g C_g + \phi_w C_w + \phi_o C_o, \\ \rho^* &= \phi_m \rho_m + \phi_g \rho_g + \phi_w \rho_w + \phi_o \rho_o, \\ \phi_m &= 1 - \phi, \quad \phi_g = \phi - (\phi_w + \phi_o). \end{aligned} \quad (5)$$

In system 5,  $C$  and  $\rho$  with respective indices “ $m$ ”, “ $g$ ”, “ $w$ ”, and “ $o$ ” denote the VHC and density for the components;  $\phi$  is the porosity. The values  $C^*$  and  $\rho^*$  in the left-hand side of system 5 are, respectively the measured VHC and density of rock. System 5 can be resolved relative  $\phi_m$ ,  $\phi_g$ ,  $\phi_w$ , and  $\phi_o$ , since the VHC and density of components are contrasting. The VHC of water is greater than that of mineral skeleton, and the VHC of water-saturated samples increases with porosity, whereas the VHC of oil- and gas-saturated rocks decreases, and a considerable difference is observed for the VHC values of rock saturated with gas, water, and oil for the whole porosity range observed for reservoir rocks.

The technique for this oil-in-place solution has been tested in laboratory. Rock samples were partially saturated with oil. The other part of the pore space was saturated with water. The density was measured with the help of the Archimedean method. Then, we calculate the VHC from these values dividing TC by TD. The TC and thermal diffusivity (TD) were measured on samples with the optical scanning method with the uncertainty up to 3% and 7%, respectively. This gives the 10-% uncertainty for VHC. Table 1 shows a comparison of theoretically derived oil saturation with experimental data. The difference between the predicted and actual values of oil saturation averages 2.5%.

Table 1. Comparison of experimental and theoretically predicted values of fluid saturation

Sample	Experimental data			Fluid content calculated		Error in oil determination, %
	Porosity, %	Relative oil saturation, %	Real oil in sample, %	Water_calc (in sample), %	Oil_calc (in sample), %	
222	23.58	85	20.04	4.11	19.47	0.57
224	20.9	65	13.59	5.63	15.27	-1.69
228	20.37	50	10.19	8.97	11.40	-1.21
233	15.85	32	5.07	7.30	8.55	-3.48
240	13.56	85	11.53	5.46	8.10	3.43
241	10.73	35	3.76	4.00	6.73	-2.97
258	13.86	50	6.93	4.76	9.10	-2.17
262	15	85	12.75	4.27	10.73	2.02
285	15.14	65	9.84	6.92	8.23	1.62
286	14.97	50	7.49	8.02	6.95	0.53
328	7.28	60	4.37	3.36	3.93	0.44

### **Interpretation of Results of TC Measurement at Elevated PT Conditions with the Help of Effective Medium Theory**

#### Analysis of Difference in Pore/Crack Geometry before and after Experiment at Elevated PT Conditions

We apply the EMT to analyze the difference in pore/crack geometry in rock samples before and after experiment at elevated PT conditions.

Two sandstone samples having initial porosity 12% and 15% are studied (Sample 1 and Sample 2, respectively). The minerals constituting the samples are as follows. Sample 1 (porosity 12%): quartz 43%, microcline 43%, calcite 10%, and clay 4%. Sample 2 (porosity 15%): quartz 53%, microcline 32%, calcite 10%, and clay 4%. The mineral composition is estimated from the thin-section analysis. The matrix TC found with the experimental-theoretical procedure before experiment at high PT conditions is 3.51 and 3.76 W/(m·K) for Samples 1 and 2, respectively. Based on thin section analysis it is assumed that the matrix TC remains unchangeable during the experiment. As seen from Figure 6a, the pores and cracks become more isometric after the experiment at elevated PT conditions; this could be explained by the effect of effective pressure (difference

between confining and pore pressure), which results in closure of thin cracks in the samples.

#### Theoretical Prediction of TC Behavior in Experiment at Elevated PT Conditions

To calculate the effective TC at elevated PT conditions, the TC of minerals and fluid are taken at the current temperature and pressure. The TC vs temperature of minerals and water used for calculations are taken from [8] and [10]. The TC of quartz decreases faster with temperature compared to that of calcite. The TC of microcline stays almost unchangeable with temperature. The clay's TC exhibits slight increase with temperature. According to our analysis of published data [11], the pressure effect on TC of minerals can be neglected. The pressure dependence of water TC in the temperature range from 20<sup>0</sup>C to 200<sup>0</sup>C is taken from [12]. In the modeling, all pressure dependences are considered with respect to the effective pressure.

It is assumed that the porosity,  $\phi$ , decreases with effective pressure according to the formula  $\phi = \phi_0 \exp(-bP_{eff})$ , where  $\phi_0$  is the porosity before the experiment at elevated PT conditions. As can be derived from the work of Kaselow and Shapiro [13], the parameter  $b$  is around 1e-4. This value depends on pore/crack geometry and should be different for different rock types. When calculating the effective TC at varying PT conditions, it was assumed that the parameters  $\alpha$  and  $\beta$  of distribution function of pore/crack volume over their aspect ratio linearly change from the values before experiment at elevated PT conditions to the values after the experiment.

The TC at elevated PT conditions is theoretically predicted for these two sandstone samples. The TC at respective PT conditions was also measured on the same samples. The comparison of normalized TC theoretically predicted and measured experimentally is shown in Figure 6b. The TC of the sample having more quartz decreases much rapidly than the TC of sample having lower quartz content. The best fit to experimental values has been produced by using the parameter  $b$  equal to 5e-3 and 1e-4 for Sample 1 and Sample 2, respectively. Since Sample 1 (initial porosity 12%) exhibits more cracks before experiment at elevated PT conditions, the porosity changes more significantly in this sample, and, respectively, the parameter  $b$  is greater for this sample compared to that of Sample 2. Analysis of Figure 6b allows one to conclude that for Sample 2, the coefficient  $b$  should be considered to be variable instead of constant, since the experimental values of normalized TC in the proximity of 60 C<sup>0</sup> are higher compared to theoretical ones. This fact can be attributed to that at the initial stage of compression, the porosity decreases faster than it is described by the constant  $b$  due to rapid closure of thin cracks. Then, the porosity closure becomes slowly and begins to satisfy the above mentioned exponential dependence with constant  $b$ .

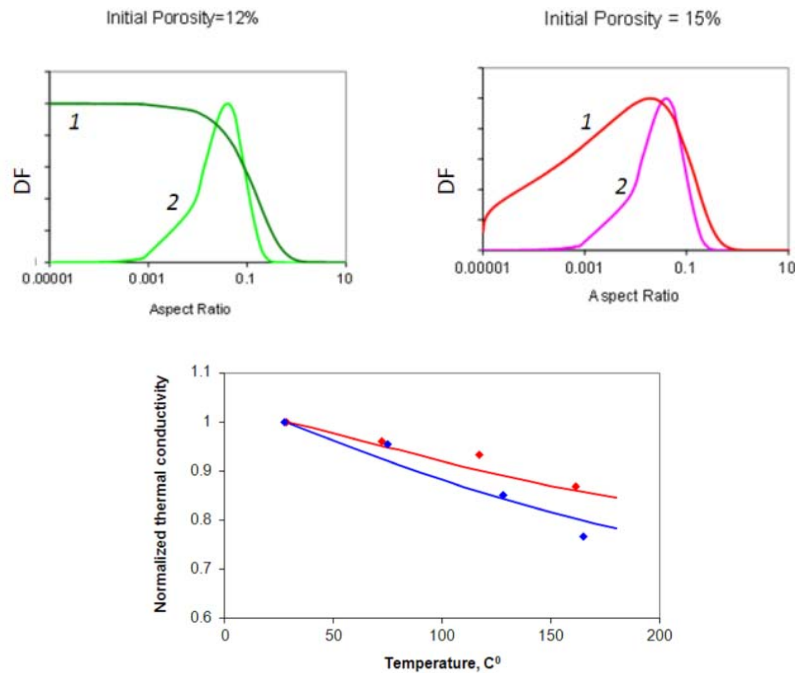


Figure 6. (a) Distribution functions of pore/crack volume over their aspect ratio before and after experiment at elevated PT conditions: 1 is distribution function before experiment, and 2 is distribution function after experiment; (b) Comparison of theoretical and experimental TC values (normalized by the TC values at standard conditions) vs temperature for sandstone samples. Upper curve shows theoretically predicted values of normalized TC for sample with initial porosity 12%, and lower curve is the theoretical prediction of normalized TC for sample with initial porosity 15%.

## CONCLUSIONS

The EMT is applied for reconstructing the matrix TC and shape of connected pores and cracks from TC measured in laboratory. The inclusion's shape inverted in the form of DFs of pore/crack volume over their aspect ratio is in good agreement with photos of pore/crack geometry of samples.

Laboratory measurements of elastic wave velocities and electrical resistivity are used for EMT-based prediction of effective TC and vice versa – the TC measurements are used to predict the velocities. The EMT-based predicted values of TC and elastic wave velocities are in good agreement with laboratory data.

The EMT is applied to predict the CLTE from pore/crack geometry that can be inverted from TC measurements and analyze its behavior versus porosity, temperature, and change of pore/crack geometry. Theoretical modeling for water saturated limestone shows that in the temperature range 20-100° C, depending on the pore/crack geometry, CLTE can vary within 20% in water-saturated isotropic limestone of 10-% porosity. Theoretical modeling of CLTE anisotropy caused by aligned cracks shows that even 1% of water-saturated cracks can produce 15-% anisotropy in CLTE of limestone.

A theoretical-experimental technique for solving the “oil-in-place” problem from measurements of density, porosity, and volumetric heat capacity has been elaborated. The technique is tested in laboratory on rocks saturated with a mixture of oil and water. The accuracy of oil saturation determination provided by the developed technique is 2.5%.

The EMT is applied to reveal principal factors governing the change of sandstone TC with pressure and temperature. For sandstones, the factors are (a) porosity change with pressure and (b) quartz content. As a result, the more rapid decrease of TC with pressure and temperature can be expected for sandstones having more quartz and greater porosity compared to other sandstones. Results of theoretical modeling based on EMT and experimental data show good agreement with results of measurements of TC of porous sandstone at elevated pressure and temperature.

## REFERENCES

1. Popov, Y., V. Tertychnyi, R. Romushkevich, D. Korobkov, and J. Pohl, “Interrelations between thermal conductivity and other physical properties of rocks: experimental data”, *Pure and Applied Geophysics*, (2003) **160**, 1137-1161.
2. Bayuk, I. and E. Chesnokov, “Correlation between elastic and transport properties of porous cracked anisotropic media”, *Phys.Chem.Earth*, (1998) **23**, 3, 361-366.
3. Chesnokov, E., I. Bayuk, and Y. Metwally, “Inversion of shale microstructure parameters from permeability measurements”, *Expanded Abstracts, 80<sup>th</sup> SEG Annual Meeting*, (2010), 2634 - 2638.
4. Landau, L. and I. Lifshitz, *Electrodynamics of Continuous Media, Second Edition: Volume 8 (Course of Theoretical Physics)*, translated from the Russian by J. B. Skyes & J. S. Bell, Pergamon Press (1982).
5. Eshelby, J., “The determination of the elastic field of an ellipsoidal inclusion and related problems”, *Proc. R. Soc. Lond. A*, (1957) **241**, 375-396.
6. Lichteneker, K. and K. Rother, “Die Herleitung des logarithmischen Mischungsgesetzes aus allgemeinen Prinzipien des stationären Strömung”, *Phys. Zeit*, (1931) **32**, 255 – 260.
7. Shermegor, T.D., *Theory of elasticity of microheterogeneous media*, Nauka, Moscow (1977) (in Russian).
8. JAHM Software “Material Properties Database MPDB v5.16”, <http://www.jahm.com> (2003).
9. Danesh, A., *PVT and Phase Behavior of Petroleum Reservoir Fluids*, Elsevier (1998).
10. Clark, S., *Handbook of Physical Constants*, Yale University, New Haven, Connecticut (1996).
11. Shoen, J.H., *Physical Properties of Rocks: Fundamentals and Principles of Petrophysics. Handbook of Geophysical Exploration. Section I, Seismic exploration: V.18*, Redwood Books, Trowbridge (1996).
12. Molchanov, A. and N. Dortman, *Petrophysics, Reference Book*, Nedra, Moscow (1992) (in Russian).
13. Kaselow, A. and S. Shapiro, “Stress sensitivity of elastic moduli and electrical resistivity in porous rocks”, *J. Geophys. Eng.*, (2004) **1**, 1 – 11.